JOURNAL OF GEOPHYSICAL RESEARCH, VOL. 103, NO. D13, PAGES 16,525–16,534, JULY 20, 1998

Changes in aerosol properties with relative humidity in the remote southern hemisphere marine boundary layer

Darrel Baumgardner

National Center for Atmospheric Research, Boulder, Colorado

Antony Clarke

Department of Oceanography, University of Hawaii, Honolulu

Abstract. In situ measurements of atmospheric aerosols have been made from an airborne platform over the remote southern hemisphere ocean in November and December 1995 as part of the First Aerosol Characterization Experiment (ACE 1). A subset of these measurements have been evaluated during three of the flights to characterize the aerosol microphysical and optical properties in the cloud-free, marine boundary. The relationship between the microphysical and optical characteristics in the size range from 0.3 to 20 μm and relative humidity was evaluated. A new technique is introduced by which the scattering coefficient is derived directly from the optical particle counter measurements. The results of this study indicate that changes in particle volume, effective radius, and optical scattering are strongly related to changes in relative humidity (RH). The observations are in very good agreement with laboratory studies of particle volume changes as a function of relative humidity.

1. Introduction

Atmospheric aerosols have a role in the direct and indirect forcing of the Earth's radiative balance as well as on photochemical and heterogeneous chemical reactions. The importance of aerosols depends on the specific microphysical and optical properties of these particles. Many factors affect how aerosols form, grow, and interact with the environment. One of the most significant factors is the relative humidity (RH) of the air that determines if aerosol particles will grow or shrink, depending upon the particle composition and magnitude of the RH [*Hanel*, 1976]. Laboratory studies, such as the large volume of work by *Tang* [1980, 1996, 1997] and *Tang and Munkelwitz* [1991, 1993, 1994] have made valuable contributions to our understanding of how aerosols behave in a controlled environment. Observational studies in the natural environment that can be compared with these laboratory studies are limited. Some measurements have been made from ground-based instrumentation in urban and continental regions [e.g., *Covert et al.*, 1980; *Rood et al.*, 1987]. Airborne measurements have been made that provide further insight into aerosol hygroscopic growth factors [*Hegg et al.*, 1996] that can be compared with the laboratory studies. One technique is to completely dry the aerosol and then subject it to a carefully controlled environment of constant RH to observe how the aerosol properties change as the RH is changed. The properties measured are usually the particle size or scattering coefficient. This technique has the advantage of minimizing the effects of too many extraneous variables from complicating the analysis. The limitation is that the sample of aerosol must be removed from its natural environment to be studied. This raises the possibility of particle losses on inlet walls [*Baumgardner et al.*, 1991]. There is also some difficulty when taking light scattering measurements made of dry aerosols measured at different RHs and applying these observations to the natural atmosphere. The process of reporting vertical profiles of light scattering coefficients from nephelometer measurements of dry aerosols requires the use of a growth factor that depends upon the assumed particle composition and vertical profiles of the RH. The atmosphere, however, is turbulent, and the RH, particularly in the boundary layer, is a quantity that varies depending upon surface fluxes and entrainment [*Moeng and Wyngaard*, 1984]. Thus it is important to understand how aerosol properties fluctuate in the natural atmosphere and to determine if these fluctuations are linked to RH variations. The remainder of this paper describes an analysis of the fluctuations of aerosol number and volume concentrations and subsequent changes in the effective radius and scattering coefficient and how these variations are linked to variations in RH.

Paper number 98JD00688.
0148-0227/98/98JD-00688$09.00

2. Instrumentation and Analysis Methodology

2.1. Measurement Systems

The C-130 aircraft, owned by the National Science Foundation, and operated by the National Center for Atmospheric Research (NCAR), was instrumented with a large array of sensors for measuring temperature, pressure, humidity, solar radiation, trace gases, and aerosol and cloud

particles. Some of the particle sensors were mounted on the wing pods and wing tips of the aircraft, while others were in the aircraft cabin, and sampled air was brought in through inlets. The majority of particle measurements discussed in this paper were made with the Forward Scattering Spectrometer Probe Model 300 (FSSP-300, Particle Measuring Systems, Inc., Boulder, Colorado) that was mounted on the right wing pod of the C-130.

The FSSP-300, whose operating principles and measurement limitations are described in detail by *Baumgardner et al* [1992], detects light that is scattered by individual particles into the forward direction between the angles of 4° to 12° as they pass isokinetically through a 0.6328 μm wavelength focused laser beam. The size of a particle is derived from the measurements using Mie scattering theory, where the particle shape is assumed spherical and the refractive index must be specified. The nominal size range that can be measured is 0.3 to 20 μm diameter. This size range varies, however, dependent upon the assumed refractive index. The sample area of the FSSP-300 is 0.05 mm2 so that a sample volume of approximately 5 cm3 $^{s-1}$ will be sampled at the typical research airspeed of 100 ms-1. The sizing uncertainty is a function of electronic roll-off, laser beam inhomogeneities, electronic noise, and calibration errors. When the refractive index is known, the calibration of the instrument can be determined accurately, and the maximum estimated uncertainty in derived size is approximately 20% [*Baumgardner et al.*, 1992]. If the refractive index is not known, however, this uncertainty increases, and the magnitude of the resultant error is dependent upon particle size. The uncertainty in number concentration is estimated as approximately 15% [*Baumgardner et al.*, 1992], and is mainly due to uncertainties in the sample volume. The sensitivity of the analysis in this paper to these errors is explored in a later section.

Table 1. Measured and Derived Parameters

Measurement	Accuracy, %
Temperature (Rosemount)	±1 [±0.1]
Pressure (Rosemount)	±.05 [±0.01]
Water Vapor (Lyman Alpha)	±2 [±0.05]
Relative humidity (derived)	±2 [±0.05]
Number concentration (FSSP-300)	±15 [±5]
Volume concentration (derived)	±38 [±10]
Effective radius (derived)	±30 [±10]
Scattering coefficient (derived)	±30 [±10]

The relative humidity reported in this analysis is calculated from the water vapor mixing ratio measured with a Lyman-Alpha hygrometer, and temperature and pressure measured

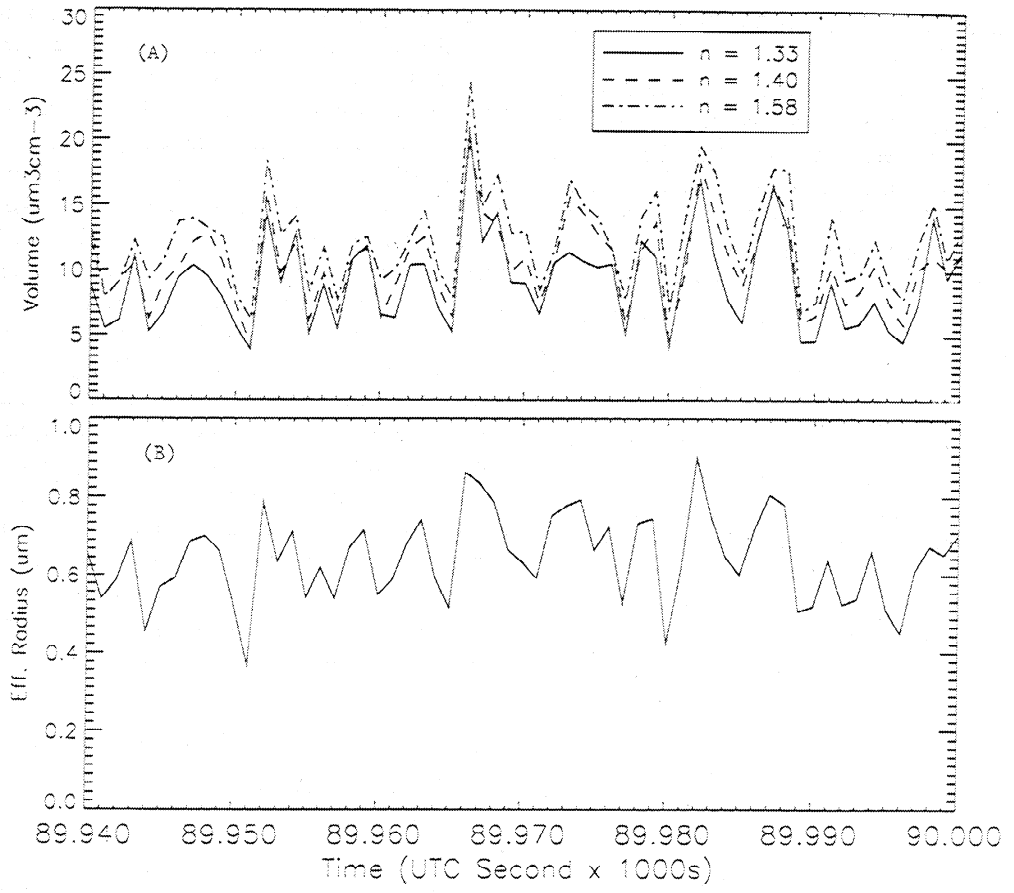

Figure 1. (a) Particle volume and (b) effective radius are calculated from the FSSP-300 measurements and shown for a small time segment during flight 24 to illustrate how volume calculations can change depending on the assumed refractive index of the particles (1.33, 1.40, and 1.58).

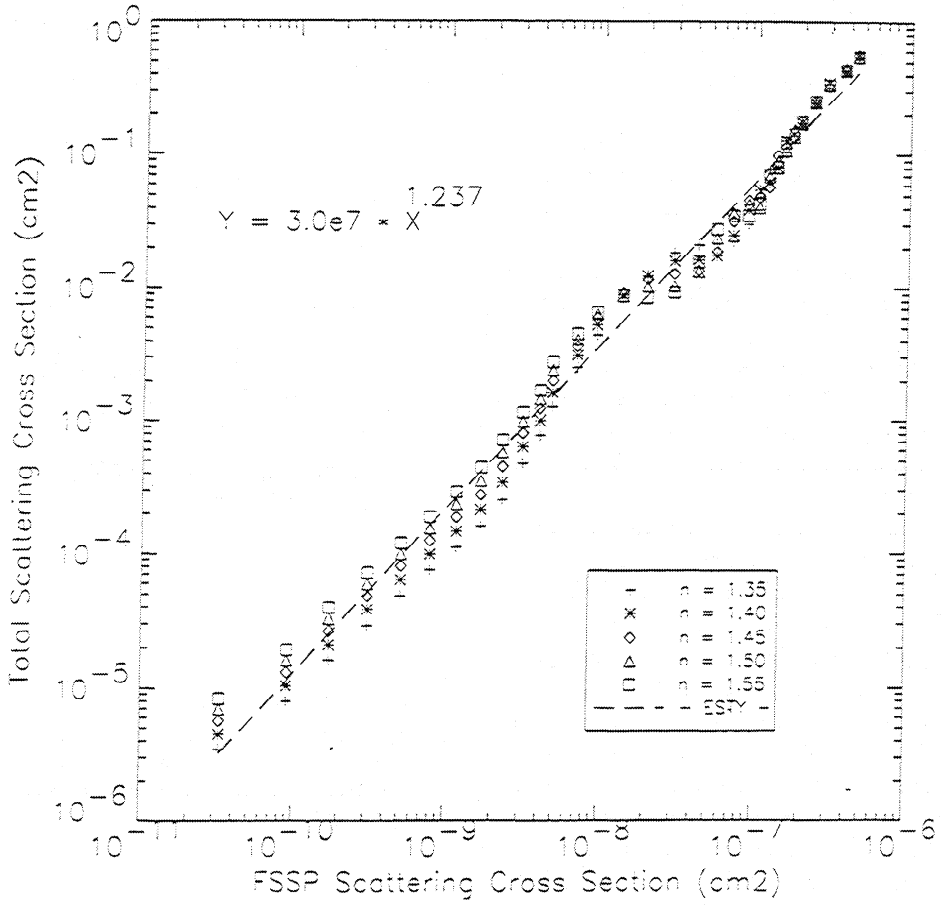

Figure 2. The scattering coefficient calculated from Mie scattering theory, assuming a wavelength of 0.6328 μm, and spherical particle is calculated for a range of particle diameters from 0.3 μm to 5.3 μm and for to values of refractive index [+ = 1.36, * = 1.42]. These values are plotted with respect to the cross section of the same-sized particles calculated with Mie theory for the scattering angles of the FSSP-300 [4°–12°].

with Rosemount (Rosemount Engineering, St. Paul, Minnesota) sensors. The Lyman-Alpha measurements are being used because this instrument responds much more quickly to moisture fluctuations than chilled mirror dew point devices. The Lyman Alpha, however, has been base-lined against the chilled mirror measurements to eliminate electronic drifts. The estimated accuracies of the water vapor, temperature, and pressure measurements are ±2, ±1, and ±.05%, respectively. Propagation of errors leads to an estimate in determining RH of ±2%. The measurements evaluated in this paper and associated uncertainties are listed in Table 1. The numbers in brackets are relative accuracies since we are more concerned in our analysis with changes in quantities rather than their absolute magnitude.

2.2 Aerosol Properties

The microphysical properties evaluated in this paper are particle number N and volume concentrations V, expressed in cm^{-3} and $\mu m^3\ cm^{-3}$, respectively. The microphysical data will be presented as average integral values of number and volume. The integral parameters are calculated from the FSSP-300 measurements by integrating over the 31 size channels, $N = \sum n_i$; $V = \pi \sum n_i d_i^3/6$, where N and V are the number and volume concentrations, respectively. The number concentration and diameter of each size category, i, are given by n_i and d_i, respectively. The diameter that corresponds to each size interval is determined from Mie scattering theory with an assumed refractive index of 1.40. This refractive index was selected as an average based upon the assumption that the majority of the particles were either sulfuric acid or some other type of sulfate particle that is at least partially deliquesced. The impact of the uncertainties discussed in the previous section, with respect to refractive index, are illustrated by Figure 1a. The volume plotted in this sample of flight data has been calculated using size thresholds on the FSSP-300 assuming refractive indices of 1.33 (water), 1.40 (deliquesced sulfate), and 1.58 (polystyrene latex calibration particles). The effect of increasing the refractive index is to increase the calculated volume. The magnitude of the differences is highly sensitive to the particle size. It can be seen when comparing Figure 1b, the effective radius, with the volume differences in Figure 1a, that these differences are largest when the effective radius is largest. A refractive index of 1.40 was selected for the remainder of the assuming a particle composition as some type of deliquesced sulfate particle at an average RH of 70%. On the basis of laboratory

studies refractive index versus RH [*Tang, I. and H.. Munkelwitz*, 1994], a value of 1.40 seemed the best compromise since we have no direct measure of the refractive index.. This assumption could lead to absolute errors of greater than 50%; however, the analysis of this paper depends upon changes in volume rather than absolute values. The uncertainty in determining relative changes is estimated at less than 20%

The optical properties that were evaluated from the FSSP-300 are σ_s^* and r_e, where σ_s^* is a surrogate of the scattering coefficient at a wavelength of 0.6328 μm and r_e is the effective radius. The effective radius is defined as the ratio of the third to the second moment of the number concentration size distribution. In order to understand what is meant by "surrogate" a brief digression is in order to describe what quantity is measured by the FSSP-300.

Optical particle counters (OPCs) do not measure the actual size of a particle. They measure the amount of light scattered into some solid angle collected by the optics. This can be interpreted as being a measure of some fraction of a single particle's scattering coefficient that is described through Mie theory as $\sigma_s^p = \pi r^2 Q_s(\lambda,\eta, r)$, where r is the particle radius and Q_s is the particle's scattering cross section at wavelength λ and refractive index η. The scattering cross section is calculated by integration of the Mie scattering function over 360°. The scattered light I, collected by the OPCs, is equal to $I_0\pi r^2 Q_s^*(\lambda,\eta, r)$, where Q_s^* is the scattering cross section of the particle over the angles of scattered light collected by the OPC, and I_0 is the intensity of laser light illuminating the particle. The calibration of the OPCs with particles of known diameter and refractive index provides the necessary scaling factor that relates I to I_0, and what is actually measured is the ratio I/I_0. Thus, we see that OPCs measure a fraction of the scattering coefficient of individual particles. By definition, an OPC can be considered as a single-particle nephelometer. This is an attractive feature since it requires no assumption about particle refractive index or size to obtain a measure of what the particle's impact might be on direct radiative forcing. The remaining question is to quantify the relationship between the surrogate and total scattering cross sections.

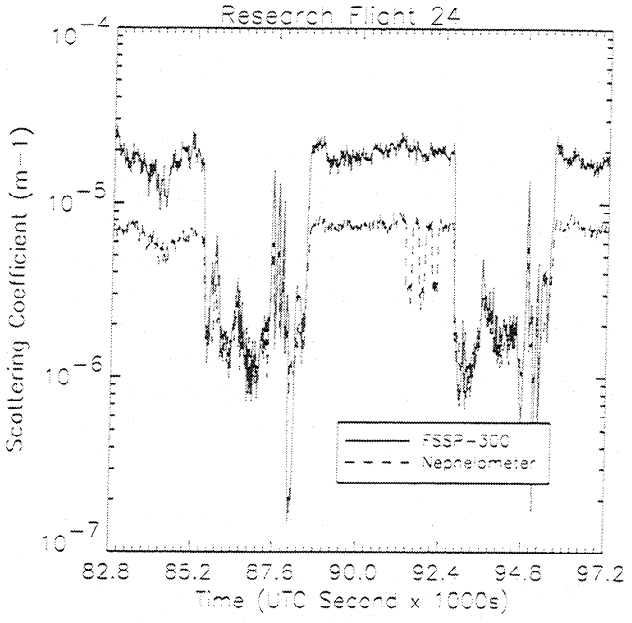

Figure 3. This time segment during flight 24 illustrates a comparison between scattering coefficient derived from the FSSP-300 using the power law relationship shown in Figure 2 and scattering coefficient measured directly with a TSI three-wavelength nephelometer. The scattering coefficient from the nephelometer is for the red wavelength.

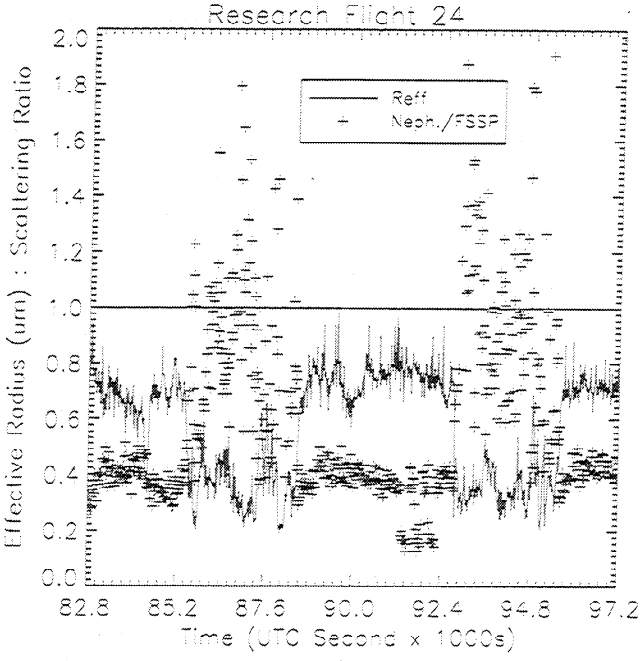

Figure 4. For the same time segment as Figure 3 during flight 24 the effective radius derived from the FSSP-300 size distributions is plotted along with the ratio of nephelometer and FSSP-300 scattering coefficients. The horizontal line at 1.0 represents perfect agreement between the two scattering measurements.

Figure 2 shows scatterplots of the theoretical coefficient of scattering as a function of the surrogate scattering coefficient for five refractive indices in the range that would be expected in the marine boundary layer [1.35-1.55] and for the FSSP-300 scattering angles of 4° to 12°. This analysis shows that the total scattering coefficient is well correlated with the scattering cross section of particles with very small dependency upon refractive index. The scattering coefficients represent particles from 0.3 to 20 μm. The relationship between the total scattering and scattering cross section, however, can be represented quite well with a simple power law equation.

As seen in Figure 2, differences in refractive index have little effect on the relationship between the total and surrogate scattering efficiencies. This is an important point since it eliminates one of the largest sources of error in deriving optical scattering from OPCs. The error in determining particle size from the FSSP-300 is approximately 20% [*Baumgardner et al., 1992*] and can be even larger depending upon uncertainties in particle refractive index and shape. The

total scattering coefficient for an ensemble of particles is

$$\sigma_s = \sum Q_s(\lambda, \eta, r) r_i^2 dn_i/dr,$$

thus uncertainties in particle size propagate by factors of 3 (including the uncertainty in cross section that is dependent upon the radius uncertainty), leading to scattering coefficient uncertainties in excess of 60%. This does not take number concentration uncertainties into account that add an uncertainty of 15%. The uncertainty in volume shown in Figure 1a reflects the differences in total scattering coefficient that would be expected as a result of refractive index uncertainties.

The total scattering uncertainty is significantly decreased when the scattering is derived directly from the measured scattering intensities. This uncertainty is a result of errors in measuring the light intensity and scaling to the total scattering values using the relationship shown in Figure 2. The error in the measurement of concentration, n_i, contributes an additional 15% uncertainty. The estimated uncertainty in measured scattering intensity for the FSSP-300 is 15% [*Baumgardner et al., 1992*], and the error of fit between the surrogate and total scattering coefficient is 20%. Propagating errors with root sum squared formulation provides an estimate of the error in estimating total extinction by this technique of approximately 30%.

The scattering coefficient at three wavelengths was also measured with a Thermo Systems Inc. nephelometer that measures the scattering from an ensemble of particles at wavelengths of 0.450, 0.550, and 0.700 μm [*Anderson et al.*, 1996]. Aerosol particles were brought into the aircraft cabin through an external inlet and dried before measurement with the nephelometer. Figure 3 shows a small segment of data where the total scattering coefficient from the nephelometer and derived from the FSSP-300 are compared. Sometimes the two measurements are in good agreement, while at other times the FSSP-300-derived values are 2-3 times larger in magnitude. This seems to be systematic and is most likely a result of scattering by larger particles. This is illustrated in Figure 4 where the effective radius calculated from the FSSP-300 is plotted along with the ratio of scattering measured with the nephelometer and FSSP-300. When the effective radius is larger, that is, greater than 0.5 μm, the FSSP-300 scattering coefficient is more than twice that measured with the nephelometer. With decreasing effective radius, however, the two scattering measurements become closer in agreement. The scattering from larger particles is underestimated by the nephelometer for three reasons. Some fraction of larger particles are lost on the walls of the inlet system because of inertial impaction [*Baumgardner et al.*, 1991] and never reach the nephelometer. The larger particles are hydrated in the boundary layer when RH values are larger than about 60%, and drying them in the aircraft will reduce their size, and hence the measured scattering. Finally, the larger particles' scattering is dominated by light scattered in the near forward direction at angles not measured by the nephelometer [*Anderson et al.*, 1996]that is, less than 7°. These near forward angles are the ones measured by the FSSP-300 and hence it is ideally suited for measuring the scattering by these larger particles. The periods in Figure 3 and 4 when the nephelometer measures more than the FSSP are when the effective radius is quite small and indicates that the scattering is probably dominated by particles below the 0.3 μm size threshold of the FSSP. This analysis indicates the need to combine the nephelometer with FSSP-300 measurements for more accurate evaluations of total light scattering.

3. Data Description and Analysis Methodology

The NCAR C-130 was stationed at Hobart, Tasmania, from November 16 to December 16, 1995. During this time period a number of flights were made to study the characteristics of aerosols over the ocean to the west and south of Tasmania. Flights 14, 17, and 24 were chosen for the analysis of this paper. The dates of these three flights were November 24, November 27, and December 7, 1995, respectively. These particular flights were selected because of the large number of flight tracks that were made at constant altitude in the marine boundary layer and away from clouds.

Table 2. Environmental Properties

Flight Leg	Date	Times	Altitude, m	Pressure, mbar	Temperature, °C	Mixing Ratio, g kg^{-1}	RH, %
1	Nov.24, 1995	24:33-24:38	648	938	5.4 [0.2]	4.3 [0.2]	70.9 [3.4]
2	Nov.24, 1995	25:53-26:10	83	1003	10.9 [0.2]	4.8 [0.3]	58.9 [3.5]
3	Nov.24, 1995	28:15-28:41	139	997	14.0 [0.3]	5.5 [0.5]	54.6 [4.8]
4	Nov.27, 1995	24:40-24:57	383	968	12.1 [0.8]	5.7 [0.5]	62.4 [4.6]
5	Nov.27, 1995	27:10-27:31	368	970	11.4 [0.7]	5.3 [0.4]	61.2 [3.6]
6	Nov.27, 1995	28:50-29:10	408	965	10.2 [0.5]	4.9 [0.3]	60.2 [3.0]
7	Dec.7, 1995	21:34-22:04	36	1009	10.8 [0.1]	6.0 [0.1]	73.8 [1.9]
8	Dec.7, 1995	22:05-22:37	150	995	9.7[0.1]	5.7 [0.1]	75.4 [1.9]
9	Dec.7, 1995	22:40-23:11	318	976	8.3[0.1]	5.3 [0.2]	75.2 [3.5]
10	Dec.7, 1995	23:13-23:43	468	958	7.3[0.1]	5.0 [0.2]	74.2 [3.9]
11	Dec.7, 1995	23:46-24:16	915	908	5.3[0.2]	3.3 [0.2]	53.4 [3.7]
12	Dec.7, 1995	24:40-25:10	29	1010	11.2[0.2]	5.9 [0.1]	71.0 [2.0]
13	Dec.7, 1995	25:12-25:44	135	997	10.1[0.1]	5.8 [0.1]	75.2 [1.9]
14	Dec.7, 1995	25:47-26:16	900	910	5.6[0.2]	3.3 [0.2]	52.7 [2.7]
15	Dec.7, 1995	26:36-27:08	28	1010	11.4[0.2]	5.9 [0.1]	70.0 [1.3]
16	Dec.7, 1995	27:11-27:41	140	997	10.3[0.1]	5.9 [0.1]	74.5 [1.5]

Table 3. Aerosol Properties

Flight Leg	Concentration, cm^{-3}	Volume, $\mu m^3\ cm^{-3}$	Effective Radius, μm	Scattering Coefficient, $m^{-1}\ x10^{-4}$
1	68 [12]	49 [51]	1.0 [0.6]	0.42 [0.10]
2	48 [7]	39 [73]	1.0 [0.8]	0.31 [0.08]
3	19 [5]	8 [13]	0.8 [0.4]	0.11 [0.05]
4	69 [14]	37 [34]	0.9 [0.4]	0.42 [0.11]
5	68 [8]	35 [41]	0.9 [0.6]	0.36 [0.09]
6	51 [7]	29 [32]	0.9 [0.5]	0.32 [0.07]
7	28 [6]	13 [0.1]	0.8 [0.1]	0.20 [0.002]
8	33 [9]	14 [10]	0.8 [0.2]	0.21 [0.06]
9	36 [18]	13 [11]	0.7 [0.3]	0.20 [0.06]
10	32 [17]	10 [6]	0.7 [0.2]	0.16 [0.05]
11	14 [21]	1 [1]	0.4 [0.2]	0.02 [0.02]
12	29 [6]	12 [10]	0.7 [0.3]	0.19 [0.05]
13	30 [4]	13 [10]	0.8 [0.2]	0.20 [0.05]
14	8 [4]	1 [3]	0.4 [0.2]	0.02 [0.02]
15	26 [4]	10 [6]	0.7 [0.2]	0.17 [0.04]

A number of soundings were made during each of the flights, and the top of the mixed layer, as observed from analysis of the potential temperature profiles, was generally about 1000 m. This varied by as much as ±200 m, depending upon the time of day and on larger-scale conditions. The results of this study are constrained to measurements made below 1000 m.

The intent of the present analysis is to evaluate fluctuations in aerosol along the flight track. Time periods were selected when the aircraft was at a constant altitude, and these periods were divided into 50 s segments (6.5 km at the average research speed of 130 ms^{-1}). Average values of the RH and particle properties were calculated for each of these 50 s segments. The differences between instantaneous and average values of the particle properties were calculated and averaged with respect to differences in RH instantaneous values from its average. The 6.5 km averaging segment was selected to match the Lagrangian length scale approximated by finding when the autocorrelation function of the particle properties was close to zero. This varied somewhat but was usually of order 50 s.

Sixteen straight and level flight legs were analyzed. Table 2 lists the times, altitudes, and average pressures, temperatures, water vapor mixing ratios, and RHs during each leg. Also given are variances, given in brackets, about the mean for these parameters. Table 3 is a similar list of means and standard deviations for the aerosol properties..

4. Results

Tables 2 and 3 show that the flight legs encountered average temperatures, pressures, mixing ratios, and RHs ranging from 5°–14°, 908–1010 mbar, 3.3–6.00 g kg^{-1}, and 53–75% , respectively, over an altitude range from 30–900 m. The N, V, r_e, and σ_s ranged from 8–69 cm^{-3}, 1–49 $\mu m^3\ cm^{-3}$, 0.4–1.0 μm, and $0.02x10^{-4}$-$0.4x10^{-4}$ m^{-1}. The range in magnitude of aerosol properties appears to be quite a bit larger than the range in environmental values. This is reflected in the variances that are also listed in the tables. Temperature, mixing ratio, and RH fluctuations are of the order of 1, 5, and 5%, respectively, of their average. On the other hand, N, V, r_e, and σ_s are approximately 25, 100, 60, and 30% of their respective averages. A comparison of the RH σ values and particle property σ values seems to show a rough positive correlation. This can be seen more clearly in Figure 5 where the aerosol property variances are plotted versus RH . Particle volume fluctuations increase most significantly with increased RH fluctuations, while r_e and σ_s show a similar trend, but to a lesser degree than the volumes. The fluctuations in aerosol concentration appear to be uncorrelated with σ variances of RH.

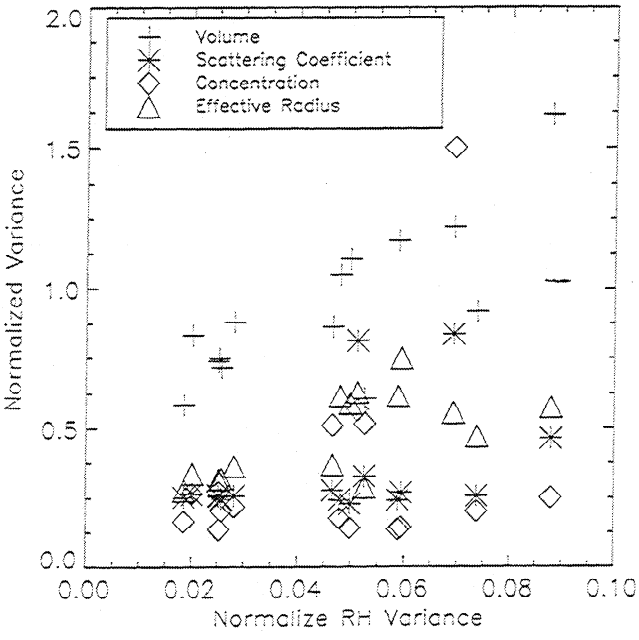

Figure 5. The variances over the 16 time segments tabulated in Tables 2 and 3 were normalized by average value over the time segment for N, V, r_e, and σ_s and are shown here plotted as a function of the normalized σ of RH.

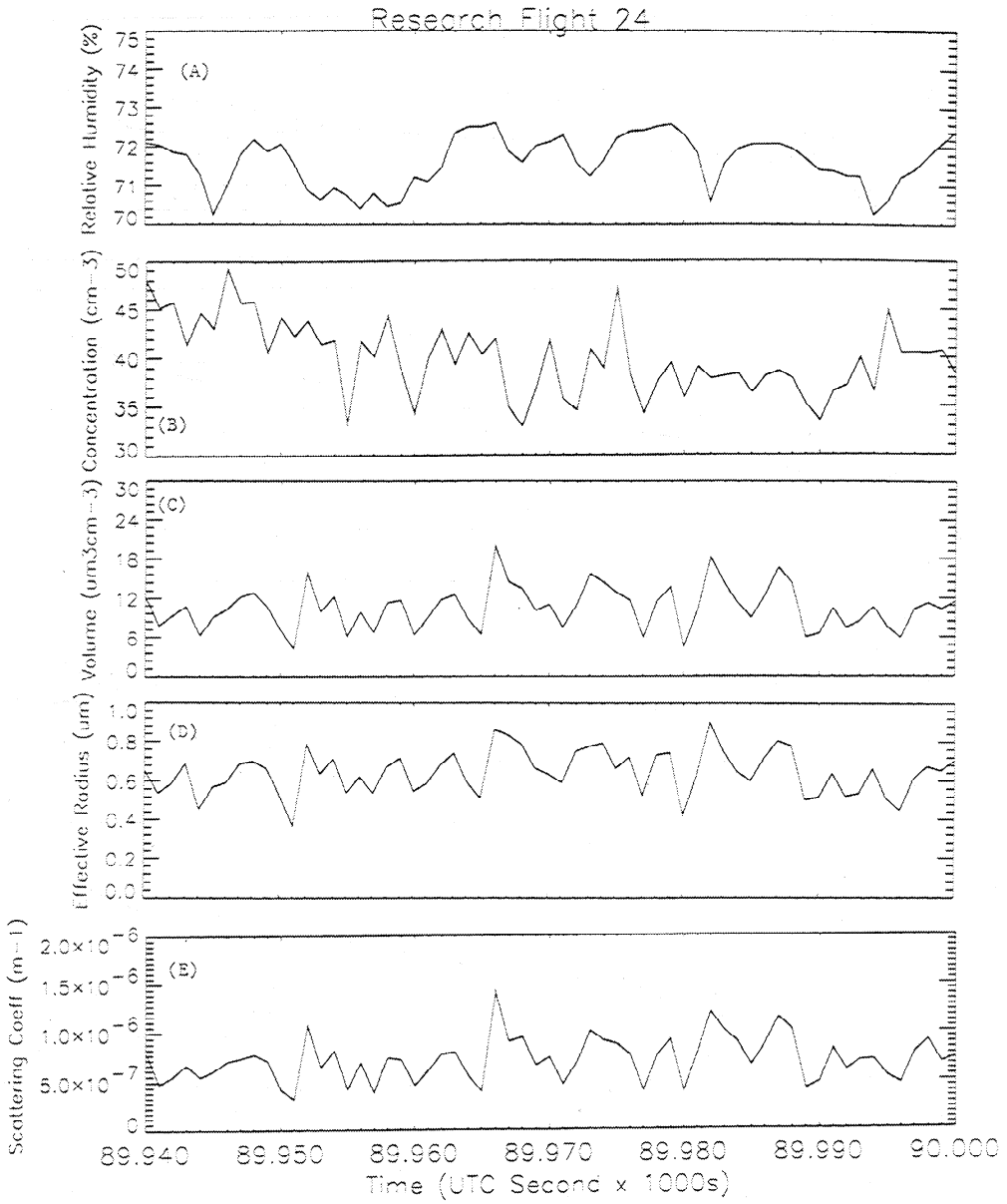

Figure 6. This 60-s segment taken from flight 24 [December 7, 1995] illustrates the fluctuations that occur in (a) RH, (b) N, (c) V, (d) r_e, and (e) σ_s. The peak to peak changes in RH, V,, r_e, and σ_s represent ±1, ±70, ±40, and ±80 of their mean values, respectively.

The correlation between RH and changes in aerosol volume is not unexpected and, as mentioned previously, has been studied in previous laboratory and field experiments. This relationship can be more clearly seen in Figure 6 where a 60-s segment of data from Flight 24 is shown. Each point represents a single, 1-s sample. The peaks and troughs of the RH plot (Figure 6a) are reflected by similar trends in N, V, r_e, and σ_s. It is unlikely that the fluctuations in these aerosol properties are a result of statistical sampling uncertainties for two reasons. First, the similarity in trends between RH and aerosol properties seems too strong to be fortuitous. Second, the average concentration in this time segment was approximately 70 cm^{-3}. The FSSP-300 samples a volume of air equal to 6.5 cm^3 in one second at 130 ms^{-1}. This means that approximately 455 particles were sampled during this time period. The statistical sampling error is ± 21 particles, or about 5%. The fluctuations observed exceed this uncertainty by a significant amount. We recognize that the 5% sampling uncertainty is only true of the total concentration and not for the concentration of each particle size. Larger particles will have lower concentrations with subsequently larger sampling uncertainties. These larger particles will also bias the volume, effective radius and scattering values derived from the FSSP. It is unlikely, however, that the sampling uncertainties are the primary cause for the ± 100% fluctuations in V seen in Figure 6c, and similar fluctuations in r_e and σ_s.

The relationship between aerosol properties and RH fluctuations was further quantified by binning the aerosol deviations as a function of RH differences. The RH categories were 0, ±2, ±4, ±6, and ±8% differences between the RH at

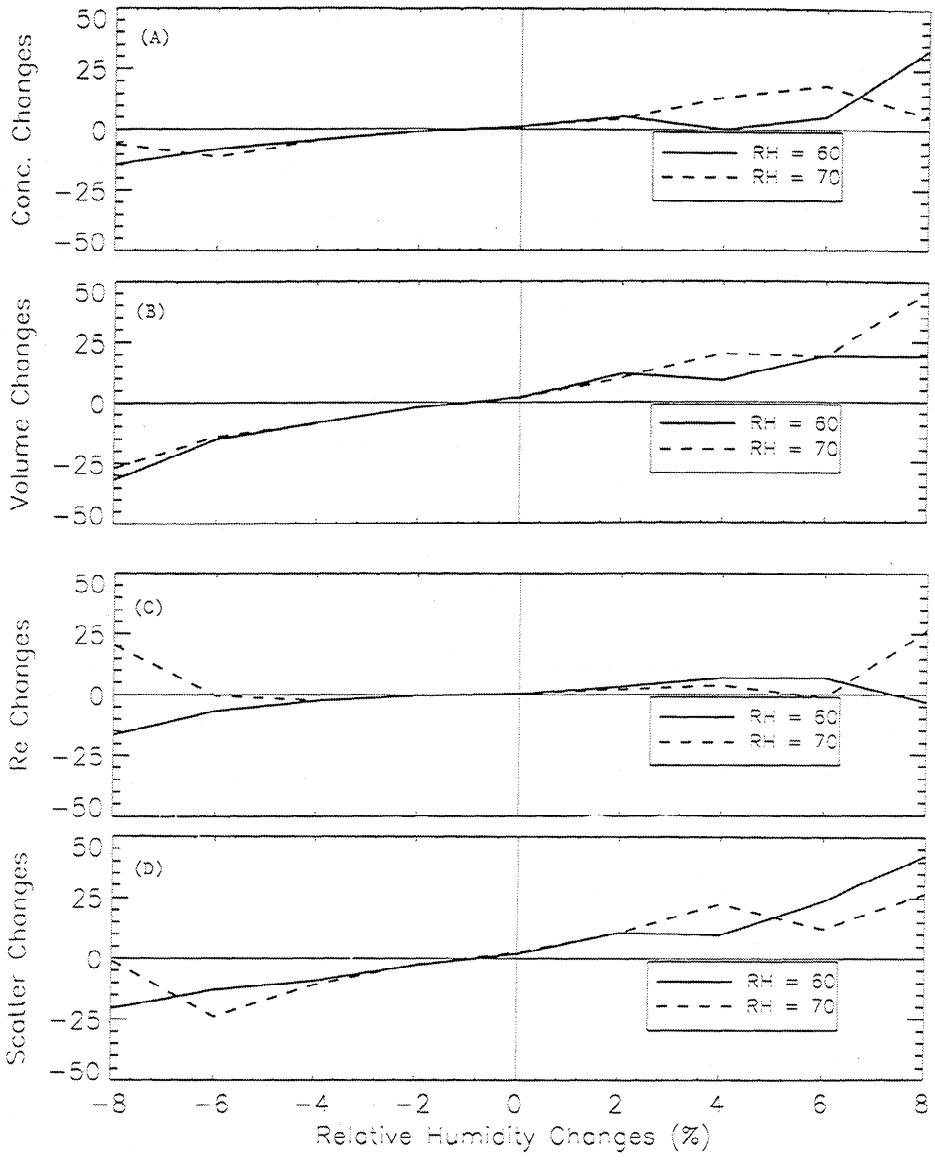

Figure 7. The 16 flight segments tabulated in Tables 2 and 3 were analyzed in 6.5 km segments by subtracting the instantaneous values (a) N, (b) V, (c) r_e, and (d) σ_s from their respective average values during the same length segment. Plotted here are these differences versus differences in RH. The 60% (solid lines) and 70% (dashed) values represent the average value of RH along a flight track.

each sample point from the average along a 6.5 km segment. The differences between instantaneous N, V, r_e, and σ_s from their averages over a flight segment were computed and averaged in the appropriate RH category. An additional stratification was done in the analysis: the data points were selected according to the average RH value along the flight segment analyzed. Figure 7 shows how the average changes in the aerosol properties relate to changes in RH for two different average values of RH, 60 and 70%. Changes in the four properties of the aerosol are positively correlated with changes in RH for both 60 and 70% RH levels. The positive fluctuations are larger for the 70% average RH than for the 60% RH, but the difference between 60 and 70% average RH on negative fluctuations is negligible. This agrees very well with expectations as will be discussed in the next section.

5. Discussion

The strong sensitivity of aerosol properties to relative humidity is expected. This study, however, can shed further light on this dependency through comparisons of the response predicted from laboratory and theoretical studies with that observed in the natural environment. The changes with humidity of V, and hence r_e and σ_s, reflect the trend predicted from laboratory studies[*e.g., Tang*, 1997]. For example, from his Figure 1, the changes in particle volume at 65, 70, and 75% RH are factors of 1.8, 2.0, and 2.2 for Na_2SO_4 particles, and factors of 3.0, 3.3, and 3.8 for NaCl. The factors here are expressed as the ratio of the volume of a dry particle to its volume at a particular RH value. If a particle has grown to some volume V_{70} at an RH of 70%, then a change in its

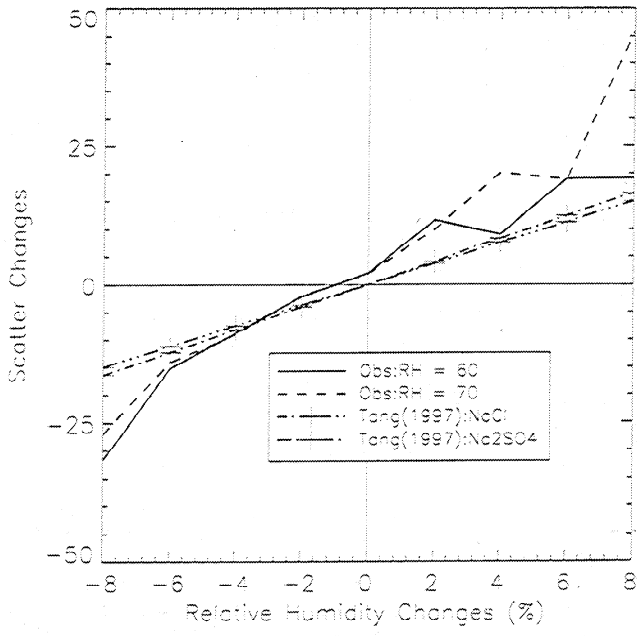

Figure 8. The volume relationship with RH shown in 7b is compared with predicted V differences from lab studies of changes in V with changes in RH [*Tang*, 1997] from the 70% average RH value.

volume to V_{65} at an RH of 65% represents a fractional change in volume of -10% for Na_2SO_4 and -9% for NaCl. Figure 8 shows comparisons between the ACE observations and the volume changes that would be predicted from the laboratory measurements of *Tang* [1997] for assumed compositions of NaCl and Na_2SO_4. If the offset in the observations at an RH change of zero is taken into account, the agreement between laboratory measurements and observations is excellent in the range of RH changes of ±2%. As RH changes by a larger amount, the observations show wider deviations than predicted by the measurements. From Table 1, the expected uncertainty in determining changes in RH and V are 0.05 and 10%, respectively. The differences between field observations and laboratory measurements are outside of this uncertainty. This may indicate that the particle composition may be something other than NaCl or Na_2SO_4. There is, however, a more likely explanation that can be understood by observing how N changes with changes in RH in Figure 7a. There is no physical reason that new particles larger than 0.3 μm (the lower threshold of the FSSP-300) should appear or disappear as humidity increases or decreases. The explanation is that particles below the size threshold of the FSSP-300 grow with increasing RH until they can be detected by the OPC. This biases the measurements by introducing new particles rather than just increasing the volume of already present aerosols. The newer particles will also bias r_e to smaller sizes and will suppress changes with RH. This is clearly seen in Figure 7c where r_e is increasing as RH increases but decreases when N is seen to sharply increase. Thus almost 20% of the increases in volume are due to newly detected particles as registered by the 20% increase in N. When this 20% is subtracted from the volume increases, it brings the changes in V to within 10% of the laboratory predictions.

The results from this study have practical applications when investigating the behavior of aerosols in the atmosphere and their subsequent impact on other atmospheric processes. The heat, moisture, and momentum of the environment must be evaluated as dynamically changing variables that depend upon turbulent diffusion and entrainment to transport them through the boundary layer. Aerosols are transported by these same mechanisms and must be evaluated with similar techniques. The analysis of the current study shows that variances in the microphysical and optical properties of aerosols are closely correlated with variances in the relative humidity. This implies that turbulent diffusion models that diagnose and prognosticate the transport of heat, moisture, and momentum can also be used to predict how aerosol characteristics will behave under varying meteorological conditions. This is demonstrated in Figure 9 where the variances in RH, V, r_e, and σ_s have been nondimensionalized [*Moeng and Wyngaard*, 1984] with the scaling variable $\langle cw \rangle^2/w_*$ and plotted as a function of altitude scaled with the height of the planetary boundary layer, in this case assumed to be 1000 m. The brackets denote the average over the covariance in fluctuations of some variable c and vertical velocity w. The variable w_* is the convective velocity scale that is taken to be approximately unity in this case. The behavior of the four variables in Figure 9 demonstrate that the aerosol variances are indeed integrally linked to variances in RH that occur as a function of altitude.

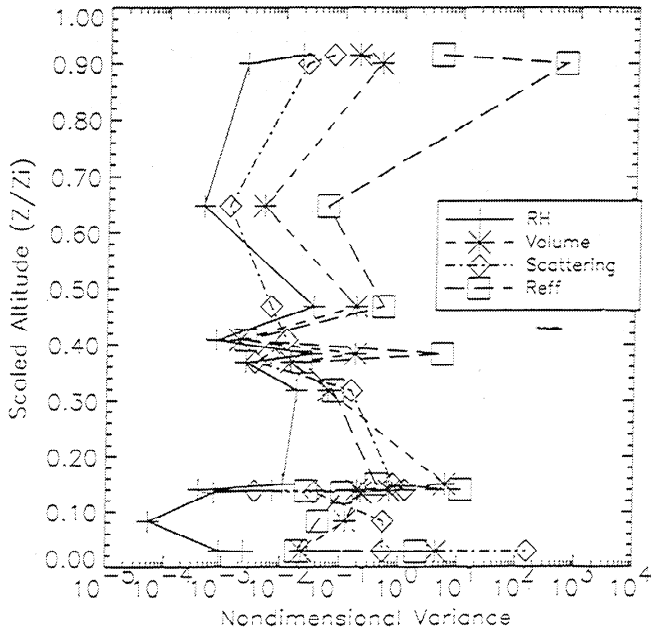

Figure 9. The variances computed along each of the flight tracks tabulated in Tables 2 and 3 for RH, V, r_e, and σ_s are normalized and shown as a function of altitude to illustrate the coupling between variances in RH and aerosol properties.

6. Summary

In situ observations of the concentration, volume, effective radius, and scattering coefficients of aerosols in the marine boundary layer over the remote southern hemisphere ocean have been analyzed to quantify the relationship between these aerosol properties and changes in relative humidity. A new analysis technique was introduced by which an OPC is used directly as a single-particle nephelometer to derive scattering coefficients a factor of 2 more accurate than the former method of obtaining this coefficient. Comparisons of the OPC-derived scattering coefficient with a commercial nephelometer that measured aerosols sampled with an inlet indicate that scattering coefficients can be significantly underestimated if particles are large or have a significant amount of water on them.

The evaluation of aerosol properties on scales of 130 m show that the volume, effective radius, and scattering coefficients have fluctuations that exceed their mean by 50% or more. These fluctuations are highly correlated with fluctuations in relative humidity. The observations of particle volume changes with RH changes agree very well with predictions based on laboratory studies.

This study has demonstrated that the variances of aerosol microphysical and optical properties can be quantified and linked to variances in RH. The implication is that climate models can take these results and parameterize them with similar techniques used to predict variances in moisture, heat, and momentum. Such parameterizations will allow a more accurate representation of aerosol properties in these models and a subsequent improvement in predicting how they impact the radiative properties of the atmosphere.

Acknowledgments. This research is a contribution to the International Global Atmospheric Chemistry (IGAC) Core Project of the International Geosphere-Biosphere Programme (IGBP) and is part of the IGAC Aerosol Characterization Experiments (ACE). The author would also like to thank the excellent flight crew and project support staff who made these measurements on the C-130 possible.

References

Anderson, T. *et al.*, Performance characteristics of a high-sensitivity, three-wavelength, total scatter/backscatter nephelometer, *J. Atmos. Oceanic Technol.*, *13*, 967-986, 1996.

Baumgardner, D., B. Huebert, and C. Wilson, Meeting Review: Airborne aerosol inlet workshop, *NCAR Tech. Note TN-362+1A*, 288 pp., Natl. Cent. for Atmos. Res., Boulder, Colo., 1991.

Baumgardner, D., J.E. Dye, R.G. Knollenberg, and B.W. Gandrud, Interpretation of measurements made by the FSSP-300X during the Airborne Arctic Stratospheric Expedition, *J. Geophys. Res.*, *97*, 8035-8046, 1992.

Covert, D.S., A.P. Waggoner, R.E. Weiss, N.C. Ahlquist, and R.J. Charlson, Atmospheric aerosols, humidity, and visibility, in *The Character and Origins of Smog Aerosols*, edited by G.M. Hidy et al., John Wiley, New York, 1980.

Hanel, G., The properties of atmospheric aerosol particles as function of the relative humidity at thermodynamic equilibrium with the surrounding moist air, *Adv. Geophys.*, *19*, 73-188, 1976.

Hegg, D.A., D.S. Covert, M.J. Rood, and P.V. Hobbs, Measurements of aerosol optical properties in marine air, *J. Geophys. Res.*, *101*, 12,893-12,903, 1996.

Moeng, C.H. and J.C. Wyngaard, Statistics of conservative scalars in the convective boundary layer, *J. Atmos. Sci.*, *41*, 3161-3169, 1984.

Rood, M.J., D.S. Covert, and T.J. Larson, Hygroscopic properties of atmospheric aerosols in Riverside, CA, *Tellus, Ser. B*, *39*, 383-397, 1987.

Tang , I.N., Deliquescence properties and particle size change of hygroscopic aerosols, in *Generation of Aerosols*, edited by K. Willeke, chap. 7, Butterworth-Heinemann, Newton, Mass.,1980.

Tang, I.N., Chemical and size effects of hygroscopic aerosols on light scattering coefficients, *J. Geophys. Res.*, *101*, 19,245-19,250, 1996.

Tang, I.N., Thermodynamic and optical properties of mixed-salt aerosols of atmospheric importance, *J. Geophys. Res.*, *102*, 1883-1893, 1997.

Tang, I.N. and H.R. Munkelwitz, Simultaneous determination of refractive index and density of an evaporating aqueous solution droplet, *Aerosol Sci. Technol.*, 15,201-15,207, 1991.

Tang, I.N. and H.R. Munkelwitz, Composition and temperature dependence of the deliquescence properties of hygroscopic aerosols, *Atmos. Environ.*, *27*, Part A, 467-473, 1993.

Tang, I.N. and H.R. Munkelwitz, Water activities, densities and refractive indices of aqueous sulfates and sodium nitrate droplets of atmospheric importance, , *J. Geophys. Res.*, *99*, 18,801-18,808, 1994.

D. Baumgardner National Center for Atmospheric Research, Research Aviation Facility, Box 3000 Boulder, CO 80307. (darrel@ncar.ucar.edu)

A. Clarke, Dept of Oceanography; University of Hawaii; Honolulu, HI 96822. (tclarke@soest.hawaii.edu)

(Received June 18, 1997; revised February 11, 1998; accepted February 18, 1998.)